

MAMBA: AN EFFECTIVE WORLD MODEL APPROACH FOR META-REINFORCEMENT LEARNING

Anonymous authors

Paper under double-blind review

ABSTRACT

Meta-reinforcement learning (meta-RL) is a promising framework for tackling challenging domains requiring efficient exploration. Existing meta-RL algorithms are characterized by low sample efficiency, and mostly focus on low-dimensional task distributions. In parallel, model-based RL methods have been successful in solving partially observable MDPs, of which meta-RL is a special case. In this work, we leverage this success and propose a new model-based approach to meta-RL, based on elements from existing state-of-the-art model-based and meta-RL methods. We demonstrate the effectiveness of our approach on common meta-RL benchmark domains, attaining greater return with better sample efficiency (up to $15\times$) while requiring very little hyperparameter tuning. In addition, we validate our approach on a slate of more challenging, higher-dimensional domains, taking a step towards real-world generalizing agents.

1 INTRODUCTION

There is a growing interest in applying reinforcement learning (RL) agents to real-world domains. One requirement of such applications is for the agent to be able to generalize and solve scenarios beyond its training data. Meta-reinforcement learning (meta-RL) is a line of work aiming to allow RL agents to generalize to novel task instances, attempting to learn a general control policy over a family of tasks. The term meta-RL covers a wide range of approaches (Duan et al., 2016; Finn et al., 2017; Nagabandi et al., 2018; Zintgraf et al., 2019) which have produced increasingly impressive results in recent years.

One line of work aiming to solve meta-RL problems is *context-based* meta-RL (Rakelly et al., 2019; Zintgraf et al., 2019; 2021). These algorithms encode trajectories of training tasks in a *context* or *belief* variable, and infer it from data at test time in order to identify the task at hand and solve it. This approach is Bayesian in nature, attempting to balance exploration (to identify the task parameters) and exploitation (to succeed in the current task). While state-of-the-art results have been reported on simulated robotic domains (Zintgraf et al., 2021; Hiraoka et al., 2021), previous meta-RL methods tend to be sample inefficient, as they rely on model-free RL algorithms. In addition, they have mostly been shown to succeed on low-dimensional task distributions.

Model-based RL is known to be more sample-efficient than its model-free counterpart (Janner et al., 2019; Ye et al., 2021). By their nature, model-based RL algorithms may also be more flexible, as they learn a model of the environment and use it to plan or learn policies, instead of learning control policies by directly interacting with the environment. A recent line of work in model-based RL has proposed Dreamer, an approach which has shown versatility to a variety of domains (Hafner et al., 2019a; 2020; 2023). Dreamer has delivered the sought-after sample efficiency of model-based RL on a variety of domains, while requiring very little hyperparameter tuning. In addition, due to its recurrent latent encoding of trajectories, it has been successful in solving partially observable Markov decision process (POMDP) scenarios (Hafner et al., 2020; 2023), which can be viewed as a general case of the context-based meta-RL formulation (where the context identifying the task is unobserved by the agent). In light of its favorable properties, we believe that Dreamer is a good fit for meta-RL. Therefore, in this work we propose to use Dreamer to solve meta-RL scenarios. To the best of our knowledge, this is the first use of the Dreamer architecture in meta-RL.

We compare Dreamer to state-of-the-art meta-RL algorithms (Zintgraf et al., 2019; 2021), and propose MAMBA (for **MetA**-RL **Model-Based** Algorithm), an algorithm leveraging the best compo-

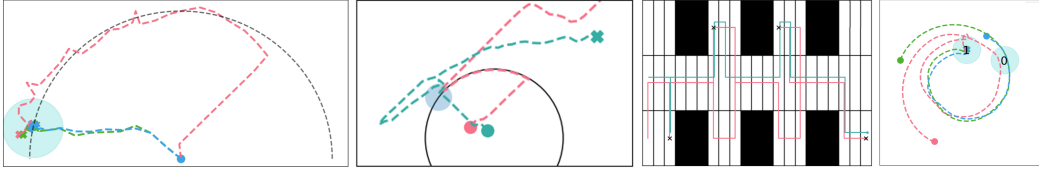


Figure 1: Behaviors learned by MAMBA in various domains. In all of the figures, the first, second and third episodes are shown in red, green and blue, respectively. From left to right: Point Robot Navigation, Escape Room, Rooms- N and Reacher- N (plotted point represents the end-effector; see Sec. 4 for details). As the environments have sparse rewards, MAMBA evidently learns near-Bayes-optimal behavior: it explores the environment on the first episode and exploits the information on the rest. For additional visualizations see <https://sites.google.com/view/mamba-iclr2024>.

nents of each. MAMBA outperforms meta-RL and model-based RL baselines on several well-studied meta-RL benchmarks, both in terms of task success and in sample efficiency. In addition, we propose a new class of challenging meta-RL domains with high-dimensional task distributions, which can be decomposed into lower-dimensional sub-tasks. By bounding the number of tasks required to obtain near-Bayes-optimal behavior (based on the analysis of Rimón et al. 2022), we show that the ability to decompose the task into sub-tasks is crucial for solving such domains efficiently. We then empirically show that MAMBA can decompose the problem better than existing meta-RL approaches, which leads to significantly better performance.

To summarize, our main contributions are:

1. We present a shared formulation of context-based meta-RL algorithms and the Dreamer line of work, highlighting their similarities and differences.
2. We develop MAMBA, a sample-efficient meta-RL approach which outperforms a variety of baselines on meta-RL benchmarks, while requiring very little hyperparameter tuning.
3. We highlight an interesting class of meta-RL environments with many degrees of freedom that is difficult for existing meta-RL methods to solve. We analyze these domains theoretically, and demonstrate the ability of MAMBA to solve them efficiently.

2 BACKGROUND

In this section we present background on partially observable Markov decision processes (POMDP) and meta-RL (Sec. 2.1). Next, we describe context-based algorithms and model-based RL (Sec. 2.2), which are popular approaches for solving meta-RL and POMDPs respectively.

2.1 PROBLEM FORMULATION

Partially observable Markov decision processes (POMDPs, Cassandra et al. 1994) are sequential decision making processes defined by a tuple $(\mathcal{S}, \mathcal{A}, \rho_0, P, R, T, \Omega, O)$, where \mathcal{S} and \mathcal{A} are the state and action spaces respectively. The process is initialized at a state sampled from the initial state distribution $s \sim \rho_0$ and evolves according to the Markovian state transition probability $P(s'|s, a)$ and reward function $R(r|s, a)$ for T time steps. The states are unobserved by the agent, which has access to observations from the observation space Ω , sampled at each time step from $O(o|s)$. Let $\tau_t = (o_0, a_1, r_1, o_1, \dots, a_t, r_t, o_t)$ be the history up to time step t . The objective is to learn a policy $\pi(a_{t+1}|\tau_t)$ which maximizes the expected return $J^\pi = \mathbb{E}_{\pi, P, O} \left[\sum_{t=1}^T r_t \right]$, where $\mathbb{E}_{\pi, P, O}$ denotes the expectation with respect to the policy, observation function and the POMDP transitions.

In **meta-reinforcement learning (meta-RL)** we consider a distribution $p(\mathcal{M})$ over a space of MDPs \mathcal{M} , where every MDP is a tuple $(\mathcal{S}, \mathcal{A}, \rho_0, P_M, R_M, T, K)$. Here \mathcal{S} and \mathcal{A} are the state and action spaces respectively, shared among all MDPs, while $P_M(s'|s, a)$ and $R_M(r|s, a)$ are the MDP-specific transition and reward functions. The agent plays K consecutive episodes in the same MDP, each consisting of T time steps. The full horizon $H = K \cdot T$ comprises the *meta-episode*, with each of its K sub-trajectories denoted *sub-episodes*. The objective is to learn a policy $\pi(a_{t+1}|\tau_t)$

which maximizes the expected return $J^\pi = \mathbb{E}_{M \sim p} \left[\mathbb{E}_{\pi, M} \left[\sum_{t=1}^H r_t \right] \right]$. Meta-RL can be seen as a special case of a POMDP, where the unobserved components are P_M and R_M , and the transitions are *episodic* – every T time steps the state is reset.

Bayes-Adaptive MDP: Solving POMDPs is known to be intractable (Papadimitriou & Tsitsiklis, 1987). While an optimal policy is generally history dependent, a convenient representation of the optimal policy uses a sufficient summary of the history (also called sufficient statistic or information state Subramanian & Mahajan 2019). One such representation is the *belief*, $b_t = P(R, P | \tau_t)$, the posterior probability over R, P given the history of transitions up to time t . The POMDP can be cast as an MDP over the belief space, known as a Bayes-adaptive MDPs (BAMDP, Duff 2002). In BAMDP, the state s_t is augmented with the belief b_t and is denoted as the augmented state $s_t^+ = (s_t, b_t)$. Formally, the BAMDP is a tuple $(S^+, A, \rho_0^+, P^+, R^+, T)$, where S^+ is the space of augmented states, A is the original action space, and ρ_0^+, P^+ , and R^+ operate over augmented states. An optimal policy $\pi_{BO} \in \arg \max_{\pi} J^\pi$ is termed *Bayes-optimal*, and is history dependent in the general case.

2.2 CONTEXT-BASED META-RL AND MODEL-BASED ALGORITHMS FOR POMDP

Context-based meta-RL: One popular approach to solving meta-RL is to encode the observed history τ_t into a latent representation which approximates the belief at time t , b_t , and learn a belief-conditioned policy in order to maximize the return J^π .

A recently successful context-based algorithm, VariBAD (Zintgraf et al., 2019), learns b_t using a Variational Autoencoder (VAE, Kingma & Welling 2013): a recurrent neural network (RNN) encoder encodes τ_t into the latent space of the VAE which is interpreted as b_t . Unlike other VAE formulations which only reconstruct the input (namely τ_t), VariBAD reconstructs the full trajectory τ_T from b_t . Meanwhile, a policy is trained on the augmented state (s_t, z_t) using a model-free RL algorithm (PPO, Schulman et al. 2017). For stability, the gradients do not flow from the RL objective through z_t into the encoder, i.e., the belief is shaped **only** by the reconstruction signal.

Recurrent latent model-based algorithms for POMDP: Model-based RL (MBRL) algorithms model the dynamics P and rewards R given data, and then use the learned models \hat{P} and \hat{R} to imagine future outcomes and optimize a policy. This approach has been shown empirically to be very sample-efficient (Schrittwieser et al., 2020; Ye et al., 2021; Hafner et al., 2023). In particular, *latent* MBRL algorithms are an appealing approach to handle partial observability by first encoding a sequence of previous observations τ_t into a latent space $z_t \in Z$, and learning dynamics $\hat{P}(z_{t+1} | z_t, a_t)$ and rewards $\hat{R}(r_t | z_t, a_t)$ directly in the latent space. This approach offers two main advantages: first, by encoding sequences of observations we allow z_t to recall information from previous time-steps which might help with the partial observability aspect. Second, imagined rollouts used to optimize the policy are defined over a much smaller space ($|Z| \ll |\Omega|$), allowing more efficient planning.

One such family of algorithms is Dreamer (Hafner et al., 2019a; 2020; 2023). In Dreamer, the world model w is a type of RNN dubbed *recurrent state space model* (RSSM, Hafner et al. 2019b), which predicts observable future outcomes from sequences of past observations. Concretely, a random sequence of transitions of length L , $\tau_{i:i+L}$, is encoded into a latent space $z_{i:i+L}$ using the RSSM. Then, for every $t \in [i, \dots, i+L]$, Dreamer predicts from z_t the next reward r_{t+1} and observation o_{t+1} and minimizes $\mathcal{L}_{pred} = -\log w(r_{t+1} | z_t) - \log w(o_{t+1} | z_t)$.

In parallel, Dreamer trains a policy conditioned on z_t which maximizes the returns of imagined future latent-space trajectories of length N_{IMG} . Finally, as in VariBAD, gradients from the policy do not propagate through to the world model w .

3 METHOD

In this section we present MAMBA. We start by motivating two main reasons for our selection of Dreamer (Hafner et al., 2023) as the backbone of our method. First, in Sec. 3.1, we demonstrate that model-based algorithms and Dreamer in particular are in fact structurally similar to state-of-the-art meta-RL algorithms. Then, in Sec. 3.2 we explain why in some meta-RL tasks the world model learning in Dreamer is advantageous. Finally, we present MAMBA in Sec. 3.3.

3.1 COMPARING VARIBAD AND DREAMER

VariBAD is a meta-RL algorithm, while Dreamer is a model-based RL method intended to solve POMDPs. Despite that, they share many of their attributes. We next describe the commonalities and differences between them.

At the core of both algorithms lie two fundamental components: a recurrent predictor for observable outcomes and a latent-conditioned policy. The *recurrent predictor* is realized by the belief encoder in VariBAD and by the world model in Dreamer. Both encode a sequence of observations into a latent space representation z_t using a RNN structure. Then, z_t is used to predict observable outcomes such as future observations and rewards. The *latent-conditioned policy* is trained via online RL objectives by predicting actions given z_t .

Despite their similarities, there are two crucial differences between VariBAD and Dreamer. First and foremost, during training, VariBAD uses its recurrent predictor to encode *the full history* τ_H starting at the very first time step of the meta-episode, while Dreamer encodes sub-trajectories that do not necessarily start at the first time step. From a computational standpoint, this makes Dreamer less computationally demanding. However, in meta-RL scenarios it could create unnecessary ambiguity as hints regarding the identity of the MDP (namely P_M and R_M), collected during time steps predating the sub-trajectory, are ignored. We refer to this as the *encoding context*.

A second key difference is the recurrent predictor reconstruction window. In Dreamer, the world model performs *local reconstruction* (predicts a single step into the future), while VariBAD performs *global reconstruction* (predicts an entire trajectory, past and future, from every z_t).

The differences in the encoding context and the local vs. global reconstruction inspire our algorithmic improvements in MAMBA (see Sec. 3.3). Additional technical differences are described in Appendix B.

3.2 DECOMPOSABLE TASK DISTRIBUTIONS

In this section we focus on the difference in reconstruction between VariBAD and Dreamer. To this end we consider a specific family task distributions and explain why they are difficult for meta-RL algorithms to solve, by extending the theoretical analysis of Rimon et al. (2022). We then show that utilizing the decomposability of these tasks makes them amenable to a much more efficient solution. Finally, we relate this decomposability to the local reconstruction horizon, and posit that Dreamer should solve these tasks more effectively. We corroborate this in experiments (Sec. 4).

3.2.1 PAC BOUNDS

Meta-RL has been shown to scale badly with respect to the number of degrees of freedom (DoF) in the task distribution (Mandi et al., 2022). Rimon et al. (2022) devised PAC upper bounds on the Bayes-suboptimality with respect to the number of training tasks. Their bounds scale exponentially with the number of DoF of the task distribution.

Many real-world domains with high number of DoF can be decomposed into sub-tasks, each with a low number of DoF. For example, a robot may be required to solve several independent problems in a sequence. In this section we analyze this family of task distributions, which we term *decomposable task distributions* (DTD), and prove that they have significantly better PAC bounds than the general case. In addition, we demonstrate that on DTD the local reconstruction approach taken by Dreamer is advantageous compared to the global reconstruction in VariBAD.

Bounds on Bayes-suboptimality for DTD: For a task which can be decomposed to K independent tasks, each with D DoF, a naive approach (such as Rimon et al. (2022)) would lead to a bound that scales exponentially in $\mathcal{O}(C^{D \times K})$, for some constant C . However, as we demonstrate in the next theorem, a method that takes task independence into account obtains $\mathcal{O}(K \times C^D)$ regret, equivalent to solving each task independently (proofs and full details in Appendix A.1 & A.2). We follow the formulation in Rimon et al. (2022) and assume access to N samples from the prior task distribution f . We estimate f using a density estimation approach, obtaining \hat{f} , and find the Bayes-optimal policy with respect to \hat{f} , i.e. $\pi_{\hat{f}}^* \in \arg \max J_{\hat{f}}^\pi = \arg \max \mathbb{E}_{M \sim \hat{f}} \left[\mathbb{E}_{\pi, M} \left[\sum_{t=1}^H r_t \right] \right]$.

Theorem 1 (informal) *Under mild assumptions, there exists a density estimator \hat{f} which maps N samples from a decomposable task distribution to a distribution over the task space, such that with probability at least $1 - 1/N$:*

$$\mathcal{R}(\pi_{\hat{f}}^*) \leq K \cdot \mathcal{O} \left(\left(\frac{\log N}{N} \right)^{\frac{\alpha}{2\alpha+D}} \right)$$

Where \mathcal{R} is the sub-optimality with respect to the true prior distribution and α is a constant which depends on the smoothness of the prior task distribution.

The key to proving Theorem 1 is to estimate each of the sub-task distributions individually, and not the entire task distribution at once, as was suggested by Rimón et al. 2022 (which leads to bounds with exponential dependency on $D \times K$ instead of D). This theoretical result is in line with our hypothesis – *concentrating on the current sub-task (or performing local reconstruction) at each time step is crucial for DTD*.

For example, in the Rooms- N environment (see Sec 4), although the total number of DoF is N (number of rooms), the difficulty of the task does not increase, as the agent should solve each of the rooms separately. In comparison, our theorem states that a standard N -dimensional navigation goal, which has the same number of DoF, should be much harder since all DoF must be estimated at once.

3.2.2 DECOMPOSABILITY AND LOCAL RECONSTRUCTION

As described in Sec. 3.1, to learn a latent representation, VariBAD utilizes a global reconstruction approach, whereas Dreamer utilizes a local one. We hypothesize that the latter approach is better for DTD (as Theorem 1 shows that it might be worst to learn a belief for the entire task).

To test our hypothesis, we compare VariBAD with the original reconstruction loss to a variant of VariBAD reconstructing only a small window of 10 transitions around the current time-step. We evaluate the two variants on the Rooms- N environment with 4 and 5 rooms, where the agent should explore consecutive rooms, passing to the next room after solving the current one (see Sec. 4 for details). We observe that using the local reconstruction is favorable in terms of total return in both the Rooms-4 and Rooms-5 scenarios (see Sec. 4).

To further analyze this phenomenon, we visualized the reward prediction using the learned decoder in VariBAD in each state of the state space and for every encoded belief (Fig. 2). We observe that VariBAD (without local reconstruction) wrongfully predicts rewards in adjacent states to the agent (Fig. 2 top (b), (f)), and thus the agent stays in the same location without a goal (as indicated by the constant state index). In comparison, introducing local reconstruction makes the **local** reward prediction much more accurate, as indicated in Fig. 2 bottom (d), (e). However, comparing top (f) and bottom (f), local reconstruction hurts the prediction of rewards in distant states. This helps the local reconstruction agent to better focus on the goal and follow near-optimal behavior. For further quantitative analysis see Appendix E. This analysis shows the efficacy of local reconstruction in comparison to a global one on DTD, which motivates our design choices in the next section.

3.3 MAMBA: META-RL MODEL-BASED ALGORITHM

In this section we describe MAMBA, our approach incorporating the model-based Dreamer into the meta-RL settings. We base MAMBA on DreamerV3 (Hafner et al., 2023) since it was shown to be a high-performance, sample-efficient, and robust algorithm that is applicable out-of-the-box to many partially observable scenarios with various input modalities. Moreover, as described in Sec. 3.1 the RSSM (Hafner et al., 2019b) of the Dreamer architecture plays the same role as the *belief encoder* in context-based meta-RL algorithms (Zintgraf et al., 2019; 2021) allowing us to more easily transfer tools and conclusions from these algorithms into MAMBA. Finally, the world model in Dreamer learns by reconstructing a single step into the future, a preferable property compared to algorithms which use a long reconstruction horizon (Sec. 3.2). Next, we describe the modifications on top of Dreamer to create MAMBA:

Modifying trajectories to support model-based meta-RL algorithms: We augment the observations o_t with the reward and the current time-step $o'_t = [o_t, r_t, t]$; both are readily available in any environment and do not require any special assumptions. In meta-RL it is common to incorporate the

rewards into the observation (Duan et al., 2016; Rakelly et al., 2019; Zintgraf et al., 2019) as it helps in identifying the sampled MDP. As for adding t , it allows to model the reset of the environment after every T steps (see Sec. 2).

Sampling full meta-episodes: To avoid missing signals about the identity of the current MDP (see *encoding context* in Sec. 3.1), we modify Dreamer to keep track of all information from the entire meta-episode when encoding z_t using the RSSM. The original Dreamer only encodes z_t for limited random sequences of actions; it samples a trajectory τ (meta-episode) from the replay buffer, samples a random starting index t , and then encodes a fixed-length sequence of $L = 64$ transitions obtaining $z_{t:t+L}$. We emphasize that using this approach, information gathered at steps $1, \dots, t-1$ is discarded. Instead, in MAMBA, we randomly sample the meta-episode τ , and feed it in its entirety into the RSSM, obtaining $z_{1:H}$. Although this creates a computational burden, as our experiments show, this allows MAMBA to obtain superior performance to Dreamer (see Sec. 4).

To alleviate some of the computational load, after obtaining $z_{1:H}$ when optimizing the RSSM and policy we sample L indices $i_1, \dots, i_L \sim \text{Uniform}(H)$ and optimize (maximize reconstruction in the RSSM, and maximize the return for the policy) only according to z_{i_1}, \dots, z_{i_L} . Formally, let $\mathcal{L}_w(z)$ and $\mathcal{L}_\pi(z)$ be the loss functions for the world model w and the policy π from a single latent vector z . Then, in Dreamer the world-model loss is $\sum_{t=i}^{i+L} \mathcal{L}_w(z_t)$ and the policy loss is $\sum_{t=i}^{i+L} \mathcal{L}_\pi(z_t)$, while in MAMBA the world-model loss is $\sum_{t=1}^L \mathcal{L}_w(z_{i_t})$ and the policy loss is $\sum_{t=1}^L \mathcal{L}_\pi(z_{i_t})$. Thus, despite the difference in RSSM input sequence lengths (L in Dreamer and H in MAMBA), during optimization Dreamer and MAMBA are updated according to the same number of latent vectors z_t .

Scheduling the world model horizon: We found that during the initial update steps, unrolling the world model for the entire meta-episode length H is inaccurate, due to the inaccuracy of the yet-untrained RSSM. In light of this inaccuracy, we reduce the computational load by learning only from prefixes of meta-episodes $\tau_{H'}$ (where H' is the prefix length). As the world model improves, we can increase H' and roll the model out for more steps. We therefore introduce a schedule: let N_T be the total number of environment steps, and define $N_{WM} \ll N_T$. The world model horizon H' increases linearly from some initial value of $WM_{initial}$ at the start of training to the full meta-episode length H when N_{WM} environment steps are taken.

Although the three modifications from Dreamer to MAMBA may appear technical, they are motivated by the concrete differences between general POMDP and the meta-RL problem. In the following section, we show that they also lead to dramatic performance improvement in meta-RL, over both the original Dreamer and state-of-the-art meta-RL methods.

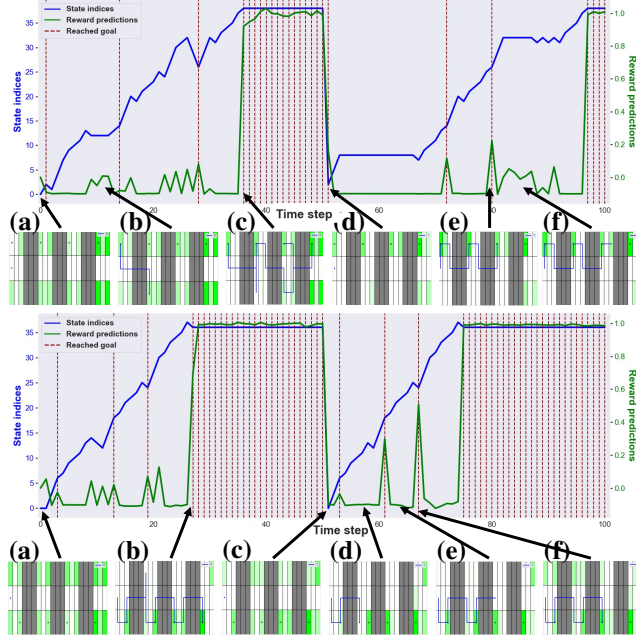


Figure 2: Reward prediction at current location (green), state identifier (blue), and goal state indication (red) through time on the Rooms-4 environment. Top: vanilla VariBAD (global reconstruction), bottom: VariBAD with local reconstruction. At the highlighted time steps (indicated by arrows) we plot the reconstructed reward for every grid cell, where positive reward prediction is represented as green, and the agent trajectory is drawn in blue.

4 EXPERIMENTS

In this section we provide an investigation of the effectiveness of MAMBA. We first show that MAMBA is a high-performing meta-RL algorithm: compared to baselines it obtains high returns with less environment steps. Next, we focus on several meta-RL scenarios including ones with sub-tasks, varying dynamics and visual observations, and show that MAMBA outperforms all baselines in each. We also investigate properties of MAMBA compared to the baselines, such as robustness to hyperparameters and the ability to utilize information from previous sub-episodes. For visualizations of our results see <https://sites.google.com/view/mamba-iclr2024>.

Environments: We use two common 2D environments in meta-RL, **Point Robot Navigation**, and **Escape Room** (Zintgraf et al., 2019; Dorfman et al., 2021; Rakelly et al., 2019). In both, a goal is randomly chosen on a half-circle and the agent must explore the circumference until it reaches it. In **Point Robot Navigation** this point is a source of positive reward, and in **Escape Room**, it is a door that leads to high rewards located outside the circle. These represent basic scenarios for varying rewards and varying dynamics in meta-RL.

Next, to test our DTD hypothesis (Sec. 3.2), we design two scenarios composed of sub-tasks, one discrete **Rooms- N** , and one continuous **Reacher- N** (where N represents the number of sub-tasks). In both tasks, a set of N goals are selected independently, and the challenge is to reach them in the correct order and memorize them between sub-episodes. Crucially, the first $N - 1$ goals only provide a positive reward once, thus encouraging the agent to find all N goals and to stay on the last one as long as possible. In **Rooms- N** the minigrid agent starts in the leftmost room and the i -th goal is on the i -th room from the left (thus the last goal is on the rightmost room). In **Reacher- N** , the agent (adopted from the DeepMind Control Suite Tunyasuvunakool et al. 2020) is a two-link robot and goals are placed in the reachable regions around it. Full details can be found in Appendix C. See Fig. 1 for visualizations of the scenarios and behaviors learned by MAMBA.

Baselines and evaluation protocol: To demonstrate the effectiveness of MAMBA, we compare it with the following baselines: two state-of-the-art meta-RL algorithms **VariBAD** and **HyperX**, an unmodified DreamerV3 which we dub **Dreamer-Vanilla**, and finally an unmodified DreamerV3 with hyperparameters identical to MAMBA, which we call **Dreamer-Tuned**. Because we tried to make MAMBA as light as possible, the hyperparameter difference between Dreamer-Tuned and Dreamer-Vanilla is in network sizes and policy imagination horizon (see Appendix D for details).

In all our experiments, we report the mean and standard deviation of four random seeds, as well as the number of environment steps each algorithm took to converge. In every experiment we test the best model seen during evaluation on a held-out test set of 1000 tasks.

MAMBA is an effective meta-RL algorithm: Our main results are described in Table 1. First, we observe that both VariBAD and HyperX, state-of-the-art algorithms specifically designed for meta-RL, perform worse than the model-based methods (both versions of Dreamer and MAMBA), both in final return and in convergence rate. This reinforces our observation regarding the similarity between both families of algorithms, and we attribute the performance gap to better algorithmic design choices in the Dreamer architecture (such as RSSM instead of simple RNN, and model-based policy optimization).

Next, we find that further fine-tuning Dreamer to meta-RL scenarios again boosts performance; focusing on Dreamer-Vanilla, Dreamer-Tune, and MAMBA, we see that it is inconclusive whether Dreamer-Vanilla and Dreamer-Tune is the better model. However, it is clearly evident that both are inferior to MAMBA. We note that the differences between Dreamer-Tune and MAMBA are algorithmic only (see Sec. 3.3), clearly demonstrating favorable algorithmic design choices in MAMBA.

Finally, we note that for the **sub-tasks scenarios** in particular, MAMBA achieves much better results than all baselines, in line with our hypothesis in Section 3.2.

Robustness of MAMBA: We evaluate robustness to hyperparameters on the Reacher-1 scenario. Here, we take three VariBAD and HyperX hyperparameter configurations from the original papers and we compare them to both Dreamer and MAMBA. The configuration of Dreamer-Vanilla was taken from Hafner et al. (2023), which is almost identical to Dreamer-Tune and MAMBA (see Appendix D). Results for their respective configurations are in Table 1. As for VariBAD and HyperX,

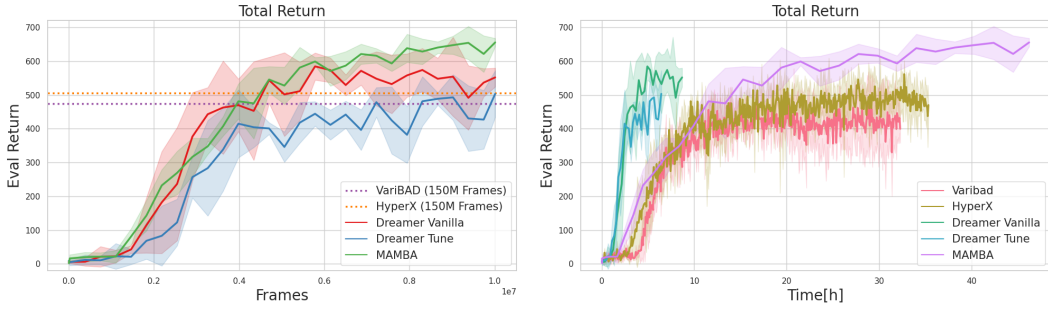


Figure 3: **Returns in Reacher:** Left: sample efficiency – meta-episode returns against the number of frames played. Since VariBAD and HyperX took $15\times$ frames to converge we show their limit instead of a full plot. Right: time efficiency – meta-episode returns against training time (hours).

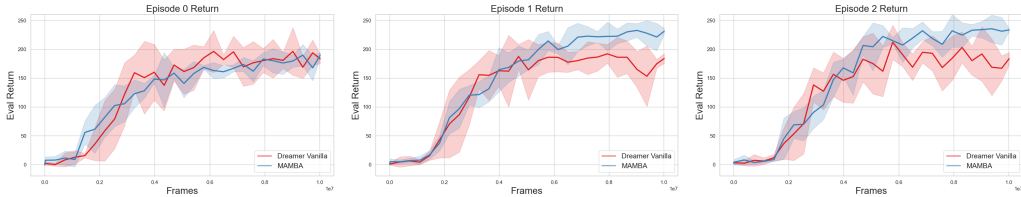


Figure 4: **Sub-episode Returns of MAMBA and Dreamer-Vanilla in Reacher** (the meta-episode contains three sub-episodes). Return of episode 0, 1, and 2, are left, middle, and right respectively. The gap between MAMBA and Dreamer demonstrates that MAMBA retains information from previous sub-episodes better than Dreamer.

Table 1 contains the best configuration which was also used for the other Reacher tasks (473.7 ± 27.5 for VariBAD, and 505.9 ± 36.0 for HyperX). The other two configurations of VariBAD achieved 104.6 ± 34.3 and 20.4 ± 2.4 . In HyperX, one configuration resulted in unstable policies obtaining arbitrarily negative returns, and the last configuration obtained 14.3 ± 0.4 . We conclude that these algorithms are highly sensitive to their hyperparameters.

This experiment hints that for new meta-RL scenarios, MAMBA and Dreamer provide good performance out-of-the-box without extensive hyperparameter tuning, while VariBAD and HyperX are more affected by hyperparameter tuning (see Figure 3, left).

Is MAMBA better at exploitation than Dreamer? In Sec. 3.3 we hypothesize that when allowing the RSSM to encode the full meta-episode, information regarding the MDP identity can be effectively retained between sub-episodes. In Fig. 4, we plot the return per sub-episode in the meta-episode. Returns for the first episode (left) are similar (hinting that both Dreamer and MAMBA learn to explore well), but MAMBA better utilizes the information gathered in previous episodes in the subsequent episodes reaching higher returns (middle and right).

Visual domain: In this scenario we leverage the ability of the Dreamer architecture to handle visual inputs. We consider the single goal Reacher scenario with two sub-episodes *with image observations*. In these settings we run each variant for 15M environment steps. We observe that Dreamer-Vanilla obtains returns of 62.7 ± 63.4 , Dreamer-Tune obtains 43.5 ± 27.0 , and MAMBA obtains 215.6 ± 64.8 , showing that MAMBA maintains superior returns in these settings as well. It is worth noting that VariBAD and HyperX in this work do not support visual inputs.

Runtime limitation: One obvious limitation of our approach is runtime – in order to recall information from the start of the meta-episode, we unroll the RSSM over the entirety of the meta-episode. In some scenarios this requires us to sequentially encode orders of magnitude more transitions.

We investigate the runtimes of each of the baselines on the Reacher scenario with a single goal. Fig. 3 (right) shows the return of each algorithm compared to the runtime of the algorithm¹. First,

¹All experiments were conducted using an Nvidia T4 GPU, with 32 CPU cores and 120GB RAM.

	VariBad	HyperX	Dreamer-Vanilla	Dreamer-Tuned	MAMBA (Ours)
HalfCircle:	218.0 \pm 26.0 ~10M	204.0 \pm 19.9 ~15M	241.1 \pm 9.9 ~2M	239.7 \pm 3.1 ~2M	242.2 \pm 7.9 ~2M
Rooms-3:	158.7 \pm 2.6	111.8 \pm 20.2	137.5 \pm 6.2	142.6 \pm 4.1	156.2 \pm 1.7
Rooms-4:	88.1 \pm 39.2	14.1 \pm 3.0	115.0 \pm 6.7	119.8 \pm 3.1	136.7 \pm 1.4
Rooms-5:	0.9 \pm 2.5	-15.8 \pm 0.4	96.5 \pm 2.5	93.9 \pm 5.3	113.1 \pm 5.7
Rooms-6:	-11.0 \pm 0.9 ~100M	-15.7 \pm 0.7 ~100M	69.5 \pm 6.3 ~6M	71.0 \pm 6.3 ~6M	94.5 \pm 1.2 ~6M
Reacher-1:	473.7 \pm 27.5	505.9 \pm 36.0	552.0 \pm 27.8	503.4 \pm 69.0	655.5 \pm 12.3
Reacher-2:	46.6 \pm 33.2	30.0 \pm 48.5	247.4 \pm 80.5	217.6 \pm 64.3	285.8 \pm 89.6
Reacher-3:	0.2 \pm 0.2	0.5 \pm 0.2	183.6 \pm 100.0	76.9 \pm 80.5	325.0 \pm 47.0
Reacher-4:	0.0 \pm 0.0 ~150M	-0.5 \pm 1.1 ~150M	0.4 \pm 0.0 ~10M	0.1 \pm 0.2 ~10M	77.7 \pm 61.1 ~10M
EscapeRoom:	70.7 \pm 5.3 ~20M	66.9 \pm 6.5 ~20M	68.2 \pm 2.4 ~4M	73.2 \pm 7.8 ~4M	73.9 \pm 3.1 ~4M

Table 1: Total return comparison of VariBad, HyperX, DreamerV3, and MAMBA on different meta environments. We report the final reward (mean \pm std), and the number of time steps until convergence (below dashed line).

we note that both Dreamer-Tune and Dreamer-Vanilla are faster than MAMBA (Dreamer-Tune is slightly faster than Dreamer-Vanilla due to reduced NN sizes). However, MAMBA is on-par or better than both VariBAD and HyperX. We think that the time gap between Dreamer and MAMBA could be further reduced, which is an interesting direction for future research.

5 RELATED WORK

Meta-Reinforcement Learning (meta-RL) has been extensively studied in recent years (Duan et al., 2016; Wang et al., 2017; Finn et al., 2017). Of specific interest to our work are context-based meta-RL approaches (Rakelly et al., 2019; Zintgraf et al., 2019; 2021), which attempt to learn a Bayes-optimal policy, and are model-free, thus suffering from high sample complexity.

Model-based RL has been shown to be more sample efficient than its model-free counterparts (Nagabandi et al., 2018; Janner et al., 2019; Schrittwieser et al., 2020; Ye et al., 2021). While there are many different approaches to model learning and usage, a prominent line of work is the Dreamer framework (Hafner et al., 2019a;b; 2020; 2023; Mendonca et al., 2021), which learns a recurrent latent space world model and uses rollouts in latent space to train a policy. This approach has been shown to work well in POMDP environments, owing to the inherent history aggregation ability of the RNN (Ni et al., 2022).

Model Based Meta-RL: Recent approaches (Nagabandi et al., 2018; Perez et al., 2020; Lin et al., 2020; Hiraoka et al., 2021) all continuously adapt to a varied task distribution, making no distinction of when a new task is attempted. In accordance, they all use short histories of states and actions, limiting usability when long horizons are required for task identification. Rimón et al. (2022); Lee & Chung (2021) learn a model of the task distribution, sampling from it to generate tasks and using these to generate full trajectories. Conversely, in our work, imagined rollouts are history-dependent, allowing the model to incorporate information from online data.

6 CONCLUSION

We present MAMBA, a high-performing and versatile meta-RL algorithm based on the Dreamer architecture. We show that MAMBA significantly outperforms existing meta-RL approaches in cumulative returns, sample efficiency and runtime. We find this result to be consistent both on common meta-RL benchmarks, on tasks with visual inputs and on a class of decomposable task distributions, for which we also provide PAC bounds. In addition, MAMBA requires little to no hyperparameter tuning.

We believe that MAMBA can be used as a stepping stone for future meta-RL research, generalizing to more challenging domains and real-world applications.

REPRODUCIBILITY

Our implementation of MAMBA is based on an open-source implementation of DreamerV3 (Hafner et al., 2023) found at <https://github.com/NM512/dreamerv3-torch>, and borrows elements from the open-source implementations of Zintgraf et al. (2019; 2021) at <https://github.com/lmzintgraf/hyperx>. All hyperparameters and details modified from the original implementation are described in the Experiments section (Sec. 4), as well as in Appendix D. In addition, we intend to publish our code once the paper is accepted.

REFERENCES

- Anthony R Cassandra, Leslie Pack Kaelbling, and Michael L Littman. Acting optimally in partially observable stochastic domains. In *Aaai*, volume 94, pp. 1023–1028, 1994.
- Era Choshen and Aviv Tamar. Contrabar: Contrastive bayes-adaptive deep rl. *arXiv preprint arXiv:2306.02418*, 2023.
- Ron Dorfman, Idan Shenfeld, and Aviv Tamar. Offline meta reinforcement learning—identifiability challenges and effective data collection strategies. *Advances in Neural Information Processing Systems*, 34:4607–4618, 2021.
- Yan Duan, John Schulman, Xi Chen, Peter L. Bartlett, Ilya Sutskever, and Pieter Abbeel. RI^2 : Fast reinforcement learning via slow reinforcement learning, 2016.
- Michael O’Gordon Duff. *Optimal Learning: Computational procedures for Bayes-adaptive Markov decision processes*. University of Massachusetts Amherst, 2002.
- Chelsea Finn, Pieter Abbeel, and Sergey Levine. Model-agnostic meta-learning for fast adaptation of deep networks. In *International conference on machine learning*, pp. 1126–1135. PMLR, 2017.
- Danijar Hafner, Timothy Lillicrap, Jimmy Ba, and Mohammad Norouzi. Dream to control: Learning behaviors by latent imagination. In *International Conference on Learning Representations*, 2019a.
- Danijar Hafner, Timothy Lillicrap, Ian Fischer, Ruben Villegas, David Ha, Honglak Lee, and James Davidson. Learning latent dynamics for planning from pixels. In *International conference on machine learning*, pp. 2555–2565. PMLR, 2019b.
- Danijar Hafner, Timothy Lillicrap, Mohammad Norouzi, and Jimmy Ba. Mastering atari with discrete world models. *arXiv preprint arXiv:2010.02193*, 2020.
- Danijar Hafner, Jurgis Pasukonis, Jimmy Ba, and Timothy Lillicrap. Mastering diverse domains through world models. *arXiv preprint arXiv:2301.04104*, 2023.
- Takuya Hiraoka, Takahisa Imagawa, Voot Tangkaratt, Takayuki Osa, Takashi Onishi, and Yoshimasa Tsuruoka. Meta-model-based meta-policy optimization. In *Asian Conference on Machine Learning*, pp. 129–144. PMLR, 2021.
- Michael Janner, Justin Fu, Marvin Zhang, and Sergey Levine. When to trust your model: Model-based policy optimization. *Advances in neural information processing systems*, 32, 2019.
- Heinrich Jiang. Uniform convergence rates for kernel density estimation. In Doina Precup and Yee Whye Teh (eds.), *Proceedings of the 34th International Conference on Machine Learning*, volume 70 of *Proceedings of Machine Learning Research*, pp. 1694–1703. PMLR, 06–11 Aug 2017.
- Diederik P Kingma and Max Welling. Auto-encoding variational bayes. *arXiv preprint arXiv:1312.6114*, 2013.
- Suyoung Lee and Sae-Young Chung. Improving generalization in meta-rl with imaginary tasks from latent dynamics mixture. *Advances in Neural Information Processing Systems*, 34:27222–27235, 2021.

- Zichuan Lin, Garrett Thomas, Guangwen Yang, and Tengyu Ma. Model-based adversarial meta-reinforcement learning. *Advances in Neural Information Processing Systems*, 33:10161–10173, 2020.
- Zhao Mandi, Pieter Abbeel, and Stephen James. On the effectiveness of fine-tuning versus meta-reinforcement learning, 2022.
- Russell Mendonca, Oleh Rybkin, Kostas Daniilidis, Danijar Hafner, and Deepak Pathak. Discovering and achieving goals via world models. *Advances in Neural Information Processing Systems*, 34:24379–24391, 2021.
- Anusha Nagabandi, Ignasi Clavera, Simin Liu, Ronald S Fearing, Pieter Abbeel, Sergey Levine, and Chelsea Finn. Learning to adapt in dynamic, real-world environments through meta-reinforcement learning. *arXiv preprint arXiv:1803.11347*, 2018.
- Tianwei Ni, Benjamin Eysenbach, and Ruslan Salakhutdinov. Recurrent model-free rl can be a strong baseline for many pomdps. In *International Conference on Machine Learning*, pp. 16691–16723. PMLR, 2022.
- Christos H Papadimitriou and John N Tsitsiklis. The complexity of markov decision processes. *Mathematics of operations research*, 12(3):441–450, 1987.
- Christian Perez, Felipe Petroski Such, and Theofanis Karaletsos. Generalized hidden parameter mdps: Transferable model-based rl in a handful of trials. In *Proceedings of the AAAI Conference on Artificial Intelligence*, volume 34, pp. 5403–5411, 2020.
- Kate Rakelly, Aurick Zhou, Chelsea Finn, Sergey Levine, and Deirdre Quillen. Efficient off-policy meta-reinforcement learning via probabilistic context variables. In *International conference on machine learning*, pp. 5331–5340. PMLR, 2019.
- Zohar Rimom, Aviv Tamar, and Gilad Adler. Meta reinforcement learning with finite training tasks—a density estimation approach. *Advances in Neural Information Processing Systems*, 35:13640–13653, 2022.
- Murray Rosenblatt. Remarks on Some Nonparametric Estimates of a Density Function. *The Annals of Mathematical Statistics*, 27(3):832 – 837, 1956. doi: 10.1214/aoms/1177728190.
- Julian Schrittwieser, Ioannis Antonoglou, Thomas Hubert, Karen Simonyan, Laurent Sifre, Simon Schmitt, Arthur Guez, Edward Lockhart, Demis Hassabis, Thore Graepel, et al. Mastering atari, go, chess and shogi by planning with a learned model. *Nature*, 588(7839):604–609, 2020.
- John Schulman, Filip Wolski, Prafulla Dhariwal, Alec Radford, and Oleg Klimov. Proximal policy optimization algorithms. *arXiv preprint arXiv:1707.06347*, 2017.
- Jayakumar Subramanian and Aditya Mahajan. Approximate information state for partially observed systems. In *2019 IEEE 58th Conference on Decision and Control (CDC)*, pp. 1629–1636. IEEE, 2019.
- Richard S Sutton, David McAllester, Satinder Singh, and Yishay Mansour. Policy gradient methods for reinforcement learning with function approximation. *Advances in neural information processing systems*, 12, 1999.
- Saran Tunyasuvunakool, Alistair Muldal, Yotam Doron, Siqi Liu, Steven Bohez, Josh Merel, Tom Erez, Timothy Lillicrap, Nicolas Heess, and Yuval Tassa. dm_control: Software and tasks for continuous control. *Software Impacts*, 6:100022, 2020.
- Jane X Wang, Zeb Kurth-Nelson, Dhruva Tirumala, Hubert Soyer, Joel Z Leibo, Remi Munos, Charles Blundell, Dharshan Kumaran, and Matt Botvinick. Learning to reinforcement learn, 2017.
- Weirui Ye, Shaohuai Liu, Thanard Kurutach, Pieter Abbeel, and Yang Gao. Mastering atari games with limited data. *Advances in Neural Information Processing Systems*, 34:25476–25488, 2021.

Luisa Zintgraf, Kyriacos Shiarlis, Maximilian Igl, Sebastian Schulze, Yarin Gal, Katja Hofmann, and Shimon Whiteson. Varibad: A very good method for bayes-adaptive deep rl via meta-learning. In *International Conference on Learning Representations*, 2019.

Luisa M Zintgraf, Leo Feng, Cong Lu, Maximilian Igl, Kristian Hartikainen, Katja Hofmann, and Shimon Whiteson. Exploration in approximate hyper-state space for meta reinforcement learning. In *International Conference on Machine Learning*, pp. 12991–13001. PMLR, 2021.

A APPENDIX

In Section A.1 we'll define the term Decomposable Task Distribution and in Section A.2 we'll show (under some mild assumptions), that we can get much more favorable bounds for these distributions compared to the general case.

A.1 DECOMPOSABLE TASK DISTRIBUTIONS

We follow the notation from Rimón et al. (2022) and assume that a task distribution is defined by a parametric space Θ , a prior distribution over this space $f \in \mathcal{P}(\Theta)$ and a mapping function from the parametric space to the MDPs space $g : \Theta \rightarrow \mathcal{M}$. To sample an MDP from the distribution, a parameter is sampled from f and is passed through g . Essentially, we assume that the distribution over MDPs can be defined as a parametric variation. This formulation is very broad and can be used to formalize all the environments considered in this paper, we refer the reader to Rimón et al. (2022) for examples and motivation. Using this formulation we can write the expected return from Section 2.1 as:

$$J^\pi = \mathbb{E}_{\theta \sim f} \left[\mathbb{E}_{\pi, M=g(\theta)} \left[\sum_{k=1}^H r_{t,k} \right] \right]$$

We next define a decomposable task distribution, namely, a task distribution where each task can be decomposed to subtasks.

Definition 1 *Decomposable Task Distribution.* Given $\{t_i, f_i, \Theta_i, g_i\}_{i=1}^{N_T}$ where $t_i \in \mathbb{N}$, $\Theta_i \subset \mathbb{R}^{d_i}$, $d_i \in \mathbb{N}$, $f_i \in \mathcal{P}(\Theta_i)$, $g_i : \Theta_i \rightarrow \mathcal{M}$ and \mathcal{M} is the MDPs space. To sample an MDP from this distribution the parameters are sampled from the priors and subtasks are being generated $\theta_i \sim f_i$, $M_i = g_i(\theta_i)$, $\forall 1 \leq i \leq N_T$. The resulting full MDP is defined by playing in M_i between time-steps t_i to t_{i+1} $\forall 1 \leq i \leq N_T$.

A.2 PAC BOUNDS USING SUB-TASK DECOMPOSITION

General Regret Bounds We first denote the well known Regret - the difference in the return of policy π to the return of the bayes-optimal policy as follows:

$$\mathcal{R}(\pi) = J^{\pi_{BO}} - J^\pi = \mathbb{E}_{\theta \sim f} \left[\mathbb{E}_{\pi_{BO}, M=g(\theta)} \left[\sum_{t=1}^H r_t \right] - \mathbb{E}_{\pi, M=g(\theta)} \left[\sum_{t=1}^H r_t \right] \right]$$

Where the π_{BO} is the bayes-optimal policy, i.e $\pi_{BO} \in \arg \max_{\pi} J^\pi$. Notice that the regret is 0 iff π is bayes optimal. Since the regret is taken with respect to the unknown prior distribution, it is a measure of the generalization of π .

In their work, Rimón et al. (2022) suggested a density estimation approach to achieve regret bounds. Assuming we get a set of N training samples, they suggested to first estimate the parametric distribution of tasks $f(\theta)$ with Gaussian Kernel Density Estimation Rosenblatt (1956)(KDE) $\hat{f}_G(\theta)$. By using KDE error bounds Jiang (2017) they achieved probably almost correct (PAC) bounds on the regret:

Theorem 2 *Theorem 6 in Rimón et al. (2022)* For a prior $f(\theta)$ over a bounded parametric space Θ that satisfies $\|f\|_\infty < \infty$ and is α -Hölder continuous, and a Gaussian KDE, we have that with probability at least $1 - 1/N$:

$$\mathcal{R}(\pi_{\hat{f}_G}^*) \leq 2R_{max}H |\Theta| C_d \cdot \left(\frac{\log N}{N} \right)^{\frac{\alpha}{2\alpha+d}}.$$

Where N are the number of sampled tasks, R_{max} is the maximum possible reward, $|\Theta|$ and d are the volume and dimension of the space Θ , respectively, C_d is polynomial with d and $\pi_{\hat{f}_G}^* \in \arg \max_{\pi} J_{\hat{f}_G}^\pi = \arg \max_{\pi} \mathbb{E}_{\theta \sim \hat{f}_G} \left[\mathbb{E}_{\pi, M=g(\theta)} \left[\sum_{t=1}^H r_t \right] \right]$, i.e the bayes-optimal policy under the assumption the estimator \hat{f}_G is correct.

This theorem shows that, given a general parametric space, the number of task samples needed to guarantee a constant regret scales exponentially with the dimension of the parametric space. This observations shows an inherit limitation of meta-RL.

Bounds for Decomposable Distributions The obvious approach to achieve regret PAC bounds in the private case of decomposable task distributions, is to take a similar approach as done in Theorem 2. We can handle the decomposable distributions as normal distributions where $\Theta_{full} = \Theta_0 \times \Theta_1 \times \dots \times \Theta_{N_T}$ and the prior distribution over the parametric space is $f^{full}(\theta = (\theta_1, \dots, \theta_{N_T})) = \prod_{i=1}^{N_T} f_i(\theta_i)$. In that case we can approximate f^{full} directly using a KDE \hat{f}_G^{full} over the samples $\{\theta_i\}_{i=1}^N$ and using Theorem 2 get regret bounds of:

$$\mathcal{R}(\pi_{\hat{f}_G^{full}}^*) \leq 2R_{max}H |\Theta^{full}| C_d \cdot \left(\frac{\log n}{n} \right)^{\frac{\alpha}{2\alpha + d^{full}}}.$$

Where $d^{full} = \sum_{i=1}^{N_T} d_i$, with d_i being the dimensionality of Θ_i . This means that if we approach decomposable task distributions as normal distributions, to guarantee a constant regret we'll need exponentially growing number of samples with respect to d^{full} , i.e depend on both the number of sub-tasks and the number of DoF in each sub-task distribution.

We suggest a different approach - estimate each distribution f_i by a KDE \hat{f}_i separately, i.e $\hat{f} = \{\hat{f}_i\}_{i=1}^{N_T}$. Next we follow the derivation of Theorem 6 in Rimón et al. (2022):

$$\begin{aligned} J_f^\pi &= \sum_{i=1}^{N_T} \mathbb{E}_{\theta \sim f_i} \left[\mathbb{E}_{\pi, M=g_i(\theta)} \left[\sum_{t=t_{i-1}}^{t_i} r_t \right] \right] = \sum_{i=1}^{N_T} \int \mathbb{E}_{\pi, M=g_i(\theta)} \left[\sum_{t=t_{i-1}}^{t_i} r_t \right] f_i(\theta) d\theta \\ J_f^\pi - J_{\hat{f}_{Sub}}^\pi &= \sum_{i=1}^{N_T} \int \mathbb{E}_{\pi, M=g_i(\theta)} \left[\sum_{t=t_{i-1}}^{t_i} r_t \right] (f_i(\theta) - \hat{f}_i(\theta)) d\theta \end{aligned}$$

And:

$$\begin{aligned} |J_f^\pi - J_{\hat{f}_{Sub}}^\pi| &\leq \sum_{i=1}^{N_T} \int \mathbb{E}_{\pi, M=g_i(\theta)} \left[\sum_{t=t_{i-1}}^{t_i} r_t \right] |f_i(\theta) - \hat{f}_i(\theta)| d\theta \\ &\leq \sum_{i=1}^{N_T} R_{max,i} \cdot (t_i - t_{i-1}) \int |f_i(\theta) - \hat{f}_i(\theta)| d\theta \end{aligned}$$

And following the same lines as the proof of Lema 3 of Rimón et al. (2022) we get:

$$\mathcal{R}(\pi_{\hat{f}_{Sub}}^*) \leq 2 \cdot \sum_{i=1}^{N_T} R_{max,i} \cdot (t_i - t_{i-1}) \int |f_i(\theta) - \hat{f}_i(\theta)| d\theta$$

Using the PAC bounds for the KDE error of Jiang (2017), as was done in Rimón et al. (2022), we receive the final regret PAC bounds:

Theorem 3 For a decomposable prior distribution $\{t_i, f_i, \Theta_i, g_i\}_{i=1}^{N_T}$ where every parametric space is bounded and $\|f_i\|_\infty < \infty$ and f_i is α -Hölder continuous $\{t_i, f_i, \Theta_i, g_i\}_{i=1}^{N_T}$. For a set of Gaussian KDEs as defined above, we have that with probability at least $1 - 1/N$:

$$\mathcal{R}(\pi_{\hat{f}_{Sub}}^*) \leq 2R_{max}H |\Theta_{max}| C_{d_{max}} \cdot \left(\frac{\log N}{N} \right)^{\frac{\alpha}{2\alpha + d_{max}}}.$$

Where N are the number of sampled tasks, R_{max} is the maximum possible reward (over all the subtasks), $|\Theta_{max}|$ and d_{max} are the maximal volume and dimensions of the spaces

$\{\Theta_i\}_{i=1}^{N_T}$, respectively, $C_{d_{max}}$ is polynomial with d_{max} and $\pi_{\hat{f}_{Sub}}^* \in \arg \max_{\pi} J_{\hat{f}_{Sub}}^{\pi} = \mathbb{E}_{\theta \sim \hat{f}_{Sub}} \left[\mathbb{E}_{\pi, M=g(\theta)} \left[\sum_{t=1}^H r_t \right] \right]$, i.e the bayes-optimal policy under the assumption the estimator \hat{f}_{Sub} is correct.

As we can see, using the fact the distribution can be decomposed into sub-distributions and approximating each one individually, resulted in a much favourable bounds. With the new approach, to guarantee a constant regret we need exponentially growing number of samples with respect to d_{max} instead of d_{full} . This essentially means that if we approach this kind of tasks by solving each sub-task individually, *the difficulty of the task will be determined by the sub-task with the highest number of DoF, and not by the number of sub-tasks.*

For example, looking at the Multi Goal Rooms N environment from our experiments, although the total number of degrees of freedom is N , i.e grows as we increase the number of rooms, the difficulty of the task does not change, as the agent should solve each of the rooms separately. In comparison, our theorem states that a standard navigation goal in N dimensions, which has the same amount of DoF will be much harder since we have estimate all the DoF at once.

Theorem 3 also sheds light on our findings from Section 3.2 that show VariBAD works better once the reconstruction window is smaller, which helps the belief (estimated by the latent vector), focus on the current sub-task.

B DIFFERENCES BETWEEN VARIBAD AND DREAMER

For simplicity, we denote VariBAD as VB, and Dreamer as D.

- **History of optimization at timestep t :** In VB, when executing the optimization at time t , the entire meta-episode gets encoded into b_t . Conversely, in D, short $L = 64$ sequences of transitions are sampled from the replay buffer and encoded into latent vectors $z_{t:t+L}$ using the RSSM world model. This is problematic in the meta context, since it doesn't allow components (policy, model, value) to depends on the full history of the meta-episode and may lead to ambiguity that should have already been resolved.
- **World model prediction horizon:** In D, the world model predicts a single step, but forces the latent states of subsequent transitions to be consistent. In VB, the decoder directly predicts outcomes (next states and rewards) for every possible observation by feeding the belief, current observation, and action as inputs to the decoder².
- **Horizon differences** In VB, episodes were short 100 timesteps, while in D, POMDPs with hundreds of timesteps were considered. This technical consideration is probably one of the factors why D samples L sub-trajectory, and why VariBAD were able to run on a GPU without out-of-memory exceptions. However, it is a limiting factor for many meta-RL tasks that are characterized with a long horizon due to the combination of several sub-episodes in every meta-episode.
- **Policy optimization:** In VB an online model-free algorithm PPO (Schulman et al., 2017) was used while D use a combination of the REINFORCE (Sutton et al., 1999) algorithm and backpropogation through imagined trajectories.
- **Policy input:** In VB, the policy is conditioned on both the latent z_t , and the current state s_t . However, in D the policy is conditioned only on z_t .
- **Hidden sizes in RNN** D has much larger hidden sizes than VB.

C FULL ENVIRONMENTS TECHNICAL DETAILS

Here we provide the full details regarding the environments we used in Section 4.

Point Robot Navigation A commonly used 2D continuous control benchmark for meta-RL (Zintgraf et al., 2019; Rimon et al., 2022; Dorfman et al., 2021; Choshen & Tamar, 2023), where a goal is

²In VariBAD, observations were not used, so an observation in this context is equal to state.

Hyper-parameter	Dreamer-Vanilla	Dreamer-Tune	Description
dyn_discrete	32	16	Number of discrete latent vectors in the world-model.
dyn_hidden	512	64	MLP size in the world-model.
dyn_stoch	32	16	Size of each latent vector in the world-model.
imag_horizon	15	10	Length of the imagination horizon (N_{IMG} cf. Sec.2.2).
units	512	128	Size of hidden MLP layers.

Table 2: Hyper parameters differences between Dreamer-Vanilla and Dreamer-Tune.

sampled on a semi-circle with radius of 1.0. The reward is sparse and defined as $1 - \|p_{agent} - p_{goal}\|_2$ when the agent is inside the goal radius (0.2) and 0 otherwise³. Here, a meta-episode consists of two sub-episodes of $K = 100$ steps each. The Bayes-optimal behavior is to explore the semicircle on the first episode and exploit the information acquired by going directly to the goal on the second.

Escape Room: In this environment, taken from Dorfman et al. (2021), a 2D point robot is initialized in a circular room of radius 1.0. An arched door of length $\frac{\pi}{8}$ is randomly sampled on the upper half of the room, provides the only exit from room. The reward is 0 inside the room and 1 outside of it. Here, a meta-episode consists of two sub-episodes of $K = 60$ steps each. A Bayes-optimal agent should explore the upper half circle, pushing against the wall until successfully exiting.

Reacher Sparse This environment, available in the DeepMind Control Suit (DMC, Tunyasuvunakool et al. 2020), is a planar two-link robot tasked to reach various goals on the plane with the tip of its second link. A goal is sampled on the 2D plane within a ball around the agent, which when reached, provides a reward proportional to the distance from the goal. For this environment we use 3 sub-episodes of length $K = 300$ for every meta-episode. In contrast to the point robot navigation task, since the goal can be sampled anywhere within the circle, the Bayes-optimal policy should explore in a spiral form to cover the entire goal space.

We also consider a variant of this task - **Multi Goal Reacher- N** (MGR- N), where N goals are sampled i.i.d. (according to the distribution above) which the robot must reach in a predetermined order. The reward for each goal $[1, \dots, N]$ may be obtained only after all the previous goals were reached. For the first $N - 1$ goals, the agent receives positive reward *only once* when the agent first penetrates the goal radius. In the N -th goal, the positive reward is given every step, until the sub-episode terminates. The Bayes-optimal behavior in this case is to explore until the last goal is found, and then stop moving. Once a goal was identified, in subsequent sub-episodes the policy should head to that identified goal directly. This serves as a high-dimensional environment decomposable into nearly independent sub-tasks, matching our analysis in Sec. 3.2. We note that for 3 and 4 goals we increased the number of steps per sub-episode to 400 instead of 300.

Multi Goal Rooms N : We consider a discrete grid-world environment consisting of a sequence of N rooms of size 3×3 separated by a 1×1 corridor. A goal is sampled in the corner of each room and the agent starts in the left-most room. The goal at room $[1, \dots, N]$ are obtainable if all the previous goals were visited. The agent receives a reward of 1 when a goal is visited, and -0.1 otherwise. For the first $N - 1$ rooms, once a goal is visited in a sub-episode, it no longer emits a positive reward. On the first sub-episode, a Bayes-optimal policy should explore each of the rooms, continuing to the next room upon finding the goal. In the second sub-episode, it should go directly to the goal in each room. This environment serves as an additional sub-task decomposable environment (see Sec. 3.2).

D HYPER-PARAMETERS OF DREAMER-TUNE

Our parameters of Dreamer-Vanilla are identical to DreamerV3 (Hafner et al., 2023). In Table 2 we list the differences between Dreamer-Vanilla and Dreamer-Tune.

	Rooms-4	Rooms-5
VariBAD Vanilla	14.1 +- 3.0	0.9+-2.5
VariBAD Local	88.1+-39.2	15.1+-13.1
MAMBA	136.7±1.4	113.1±5.7

Table 3: VariBAD reconstruction ablation study. As we can see using local reconstruction helped in the Rooms environment, which contains sub-tasks.

E EMPIRICAL RESULTS FOR VARIBAD WITH LOCAL RECONSTRUCTION

In Sec. 3.2, we introduced a variant of VariBAD that uses a local reconstruction (reconstructing a window of adjacent transitions instead of the full trajectory). In this section we evaluate it against the original VariBAD on two sub-tasks environments: Rooms-4 and Rooms-5, in Table 3. We also provide the results of MAMBA from Sec. 4 as reference.

As we can see in Table 3 local reconstruction helped VariBAD in these scenarios, which is in line with our theoretical findings (cf. Sec. 3.2).

³Inside the goal radius the rewards are positive.